Pharm Res (2013) 30:2880–2890
DOI 10.1007/s11095-013-1117-1

RESEARCH PAPER

Epigenetic Regulation of Organic Anion Transporting Polypeptide 1B3 in Cancer Cell Lines

Satoki Imai • Ryota Kikuchi • Yuri Tsuruya • Sotaro Naoi • Sho Nishida • Hiroyuki Kusuhara • Yuichi Sugiyama

Received: 5 February 2013 / Accepted: 11 June 2013 / Published online: 28 June 2013

ABSTRACT

Purpose The expression of a multispecific organic anion transporter, OATP1B3/*SLCO1B3*, is associated with clinical prognosis and survival of cancer cells. The aims of present study were to investigate the involvement of epigenetic regulation in mRNA expression of a cancer-type variant of OATP1B3 (Ct-OATP1B3) in cancer cell lines.

Methods The membrane localization and transport functions of Ct-OATP1B3 were investigated in HEK293 cells transiently expressing Ct-OATP1B3. DNA methylation profiles around the transcriptional start site of Ct-OATP1B3 in cancer cell lines were determined. The effects of a DNA methyltransferase inhibitor and siRNA knockdown of methyl-DNA binding proteins (MBDs) on the expression of Ct-OATP1B3 mRNA were investigated.

Results 5′-RACE identified the TSS of *Ct-OATP1B3* in PK-8 cells. Ct-OATP1B3 was localized on the plasma membrane, and showed the transport activities of $E_2$17βG, fluvastatin, rifampicin, and Gd-EOB-DTPA. The CpG dinucleotides were hypomethylated in Ct-OATP1B3-positive cell lines (DLD-1, TFK-1, PK-8, and PK-45P) but were hypermethylated in Ct-OATP1B3-negative cell lines (HepG2 and Caco-2). Treatment with a DNA methyltransferase inhibitor and siRNA knockdown of MBD2 significantly increased the expression of Ct-OATP1B3 mRNA in HepG2 and Caco-2.

Conclusions Ct-OATP1B3 is capable of transporting its substrates into cancer cells. Its mRNA expression is regulated by DNA methylation-dependent gene silencing involving MBD2.

KEY WORDS cancer cell line · DNA methylation · drug transporter · epigenetics · OATP1B3

ABBREVIATIONS

5′-RACE	5′-rapid amplification cDNA ends
ChIP	chromatin immunoprecipitation
$E_2$17βG	estradiol 17β-D-glucuronide
Gd-EOB-DTPA	gadolinium ethoxybenzyl diethylenetriamine pentaacetic acid
ICP-MS	inductively coupled plasma mass spectrometry
LC-MS/MS	liquid chromatography-tandem mass spectrometry
MBD	methyl-DNA binding protein
OATP	organic anion transporting polypeptide
ORF	open reading frame
PCR	polymerase chain reaction
SLC	Solute carrier
T-DMR	tissue-dependent differentially methylated region
TSS	transcriptional start site

Electronic supplementary material The online version of this article (doi:10.1007/s11095-013-1117-1) contains supplementary material, which is available to authorized users.

S. Imai · R. Kikuchi · Y. Tsuruya · S. Naoi · H. Kusuhara
Laboratory of Molecular Pharmacokinetics
Graduate School of Pharmaceutical Sciences
The University of Tokyo, Tokyo, Japan

S. Imai
Pharmacokinetics Research Laboratories
Dainippon Sumitomo Pharma Co., Ltd., Osaka, Japan

S. Nishida
Laboratory of Plant Nutrition and Fertilizers
Graduate School of Agricultural and Life Sciences
The University of Tokyo, Tokyo, Japan

Y. Sugiyama (✉)
Sugiyama Laboratory, RIKEN Innovation Center
Research Cluster for Innovation, RIKEN, 1-6 Suehiro-cho
Tsurumi-ku, Yokohama City, Kanagawa 230-0045, Japan
e-mail: ychi.sugiyama@riken.jp

INTRODUCTION

A multispecific organic anion transporter, OATP1B3/*SLCO1B3*, is predominantly expressed in the liver under physiological conditions. Together with OATP1B1, another member in the same gene family, OATP1B3 mediates the cellular entry of various endogenous compounds and numerous xenobiotics including clinically used drugs (1–5). In addition to the normal liver, OATP1B3 is also expressed in various tumors, such as gastrointestinal (6), breast (7), lung (8), colon (9), prostate (10), and ovarian cancers (11), whereas the expression of OATP1B1 in cancer cell lines or cancerous tissues has not been reported so far. The expression of OATP1B3 in tumors and cancer cell lines seems to have functional consequences. OATP1B3 immunoreactivity is associated with tumor size, a decreased risk of recurrence and improved prognosis of breast carcinomas (7). In prostatic cancer, a *SLCO1B3* haplotype (334GG/699AA) is associated with improved survival in patients (10). In contrast, overexpression of OATP1B3, but not OATP1B3 mutant (G583E) lacking the transport activity, conferred an antiapoptotic advantage against chemotherapy treatment in colon cancer cell lines (9).

We previously demonstrated that the mRNA expression of OATP1B3 in cancer cells as well as normal tissue is associated with DNA methylation status around the transcriptional start site (TSS) (12,13). CpG dinucleotides around the TSS were significantly hypomethylated in two OATP1B3-positive cell lines, DLD-1 and TFK-1, and in the liver, while hypermethylated in two OATP1B3-negative cell lines, HepG2 and Caco-2, and in the kidney. Treatment with DNA methylation inhibitor increased the mRNA expression of OATP1B3 in HepG2 and Caco-2 cells, but not in DLD-1 and TFK-1 cells. It was of note that the same region was hypermethylated in PK-8 and PK-45P cells regardless of the abundant expression of OATP1B3 mRNA. This apparently contradictory finding led us to speculate that these two cell lines utilize an alternative TSS for the transcription of OATP1B3. Recently, cancer-type OATP1B3 (Ct-OATP1B3), of which the TSS was localized in the intron 2 of *SLCO1B3* gene, was newly identified as the primary mRNA variant of OATP1B3 at least in the human cancerous tissues and cell lines examined in the study (14). Indeed, the mRNA expression level of Ct-OATP1B3 was more than 3,000-fold higher than that of Lt-OATP1B3 in PK-45P cells, where we observed a disconnect between the DNA methylation status around the TSS of *Lt-OATP1B3* and mRNA expression. It was predicted that the peptide sequence of Ct-OATP1B3 retains transporter-like structure, lacking 47 amino acids at the N-terminus of Lt-OATP1B3 (14) although its subcellular localization, and transport activities remained to be investigated. In the meantime, another group very recently confirmed the existence of Ct-OATP1B3 (OATP1B3 V1) as a predominant OATP1B3 variant in human colon cancer tissues and cell lines, and the predicted amino acid sequence in their study was identical to the one we identified (15). An effort to unveil the regulatory mechanisms underlying the expression of Ct-OATP1B3 could foster a new paradigm of tumor diagnostics (16).

The purpose of the present study was 1) to expand the previous findings about the expression and function of Ct-OATP1B3 which derives from the same gene as Lt-OATP1B3, and 2) to investigate the regulation of its mRNA expression focusing on the involvement of epigenetic systems.

MATERIALS AND METHODS

Reagents

All reagents were purchased from Wako Pure Chemicals (Osaka, Japan) unless stated otherwise. [^{3}H]Estradiol 17β-D-glucuronide ([^{3}H]$E_2$17βG) (50.1 Ci/mmol) were purchased from PerkinElmer Life and Analytical Sciences (Boston, MA). Gadolinium ethoxybenzyl diethylenetriamine pentaacetic acid (Gd-EOB-DTPA) was obtained from Bayer (Leverkusen, Germany). Antibodies against FLAG epitope, calnexin and Na^+, K^+-ATPase alpha 1 subunit were purchased from Abcam (Cambridge, UK). Anti-EEA1, anti-LAMP1 and anti-GM130 antibodies were obtained from BD Pharmingen (San Diego, CA). MitoTracker Red CMXRos were purchased from Molecular Probes (Molecular Probes, Inc., Eugene, OR).

Cell Culture

HepG2 and Caco-2 cells were obtained from American Type Culture Collection (Manassas, VA) and DS Pharma Biomedical (Osaka, Japan), respectively. DLD-1, TFK-1, PK-8, and PK-45P cells were kindly provided by the Cell Resource Center for Biomedical Research, Institute of Development, Aging and Cancer, Tohoku University, Japan. These cells were maintained as described previously (12,17). The origins of the cell lines are as follows: HepG2, hepatocellular carcinoma; Caco-2 and DLD-1, colorectal carcinoma; TFK-1, bile duct carcinoma; PK-8 and PK-45P, pancreatic carcinoma.

RNA Isolation and Real-Time PCR

Total RNA was prepared from cells or tissue specimens by a single-step guanidium thiocyanate procedure using ISOGEN (Nippon Gene, Toyama, Japan) according to the manufacturer's instructions. The RNA was then treated with DNase I (Sigma-Aldrich, St. Louis, MO) to remove the contaminated genomic DNA, followed by reverse transcription

(RT) using a random nonamer primer (Takara, Shiga, Japan). The quantitative real-time PCR was performed using 7900HT Fast Real-Time PCR System (Applied Biosystems, Foster City, CA, USA) and SDS Software version 2.3 according to the manufacturer's instructions. Primer set A and B were used for the mRNA quantification of Ct-OATP1B3 and Lt-OATP1B3, respectively (Supplementary Material Table I). These primer sets were designed not to recognize sequences of homologous genes such as OATP1B1 or OATP1B7. The protocol for PCR was as follows: 50°C for 2 min; 95°C for 10 min; 40 cycles of 95°C for 15 s and 60°C for 1 min. A standard curve was generated by dilutions of the target PCR product, which had been purified and had its concentration measured.

Identification of the Transcription Start Sites of OATP1B3 in PK-8

5′-rapid amplification cDNA ends (5′-RACE) was performed in order to determine the TSS of *SLCO1B3* gene in PK-8 cells using SMARTer^{TM} RACE cDNA amplification kit (Clontech, Mountain View, CA). Following the synthesis of first-strand cDNA from total RNA extracted from PK-8 cells according to the manufacturer's instructions, 5′-RACE PCR was performed using gene-specific antisense primers shown in Supplementary Material Table I. The protocol for PCR was as follows: 5 cycles of 94°C for 30 s and 72°C for 3 min; 5 cycles of 94°C for 30 s, 70°C for 30 s and 72°C for 3 min; 32 cycles of 94°C for 30 s, 68°C for 30 s and 72°C for 3 min. After TA cloning of the PCR product, 12 clones were picked and sequenced to determine the TSS.

Construction of Plasmid Vector Containing the Predicted Open Reading Frame (ORF) of Ct-OATP1B3

The cDNA of Ct-OATP1B3 was PCR amplified using pcDNA3.1(+)-Lt-OATP1B3 (18) as a template with a forward primer containing a NotI restriction site and Kozak sequence before the predicted translation start codon of Ct-OATP1B3 and a reverse primer containing a BamHI restriction site before the translation stop codon of Ct-OATP1B3 (Supplementary Material Table I). After digestion with the restriction enzymes, the cDNA of Ct-OATP1B3 were ligated into p3×FLAG-CMV-14 expression vector (Sigma-Aldrich, St. Louis, MO) which has been predigested with NotI and BamHI. The DNA sequences were confirmed using an ABI PRISM 3110 Genetic Analyzer (Applied Biosystems, Foster City, CA).

Immunocytochemical Staining

p3×FLAG-CMV-14-Ct-OATP1B3 vector constructed above was transfected into HEK293 cells using FuGENE HD (Roche Applied Science, Mannheim, Germany) according to the manufacturer's instructions. Forty-eight hours after transfection, the cells were fixed in PBS containing 4% paraformaldehyde for 10 min and then permeabilized in 0.1% saponin for 10 min. After blocking with 3% BSA for 30 min, the cells were incubated with goat anti-FLAG antibody and either one of the following antibodies for 2 h; mouse anti-Na^+, K^+-ATPase alpha 1 subunit antibody, mouse anti-EEA1 antibody, mouse anti-LAMP1 antibody, mouse anti-GM130 antibody, or rabbit anti-calnexin antibody. Then, the cells were incubated with Alexa Fluor 488 donkey anti-goat immunoglobulin G and Alexa Fluor 594 donkey anti-mouse or anti-rabbit immunoglobulin G (Molecular Probes, Inc., Eugene, OR) for 1 h. These staining procedures were performed at room temperature. For staining with MitoTracker, 250 nM MitoTracker Red CMXRos was added to the medium for 30 min and washed out for 10 min prior to fixation. The cells were mounted onto glass slides with VECTASHIELD mounting medium (Vector Laboratories Inc., Burlingame, CA) and were visualized by confocal microscopy using a Leica TCS SP5 II laser-scanning confocal microscope (Leica, Solms, Germany).

In Vitro Transport Study Using HEK293 Cells Expressing Ct-OATP1B3

HEK293T cells were seeded 72 h before the transport assay in poly-L-lysine- and poly-L-ornithine-coated 24-well plates at a density of 1.5×10^5 cells per well. The transfection of p3×FLAG-CMV-14-Ct-OATP1B3 vector and p3×FLAG-CMV-14-mock vector into the cells was performed using X-tremeGENE HP DNA transfection reagent according to the manufacture's protocol (Roche Applied Science). The cell culture medium was replaced with medium supplemented with 5 mM sodium butyrate 24 h before the transport assay to induce the expression of transporter proteins. The transport experiment was carried out as described previously (18). Briefly, uptake was initiated by the addition of substrates with or without rifampicin (100 μM), after the cells had been washed twice and preincubated with Krebs-Henseleit buffer at 37°C for 15 min. The Krebs-Henseleit buffer consisted of 118 mM NaCl, 23.8 mM $NaHCO_3$, 4.8 mM KCl, 1.0 mM KH_2PO_4, 1.2 mM $MgSO_4$, 12.5 mM HEPES, 5.0 mM glucose, and 1.5 mM $CaCl_2$ and was adjusted to pH 7.4. The uptake was terminated at a designated time by the addition of ice-cold Krebs-Henseleit buffer after the removal of incubation buffer. To determine the uptake of [^{3}H]$E_2$17βG, the cells were solubilized with NaOH overnight at 4°C and then neutralized with HCl, and the radioactivity in the cell specimens was measured by liquid scintillation counting. To determine the uptake of fluvastatin, rifampicin and Gd-EOB-DTPA, cells were sonicated in 200 μL of distilled water and the aliquots were used for LC-MS/MS (fluvastatin and

rifampicin) or ICP-MS quantification (Gd-EOB-DTPA) as described below. The protein concentration was determined using the method of Lowry with bovine serum albumin as the protein standard as described previously (19). The uptake was expressed as distribution volume, representing the amount associated with cells specimens divided by the substrate concentration in the medium. For comparison, uptake study of fluvastatin and rifampicin using HEK293 cells expressing Lt-OATP1B3 (18) was also performed.

Quantification of Drug Concentrations by LC-MS/MS

Fifty μL of aliquots obtained from the uptake study were protein precipitated by adding 100 μL of acetonitrile, mixed and centrifuged at 15,000 rpm for 5 min. The supernatants (75 μL) were mixed with 175 μL of 0.1% formic acid and an aliquot was used for LC-MS/MS analysis. An AB SCIEX QTRAP 5500 mass spectrometer (Applied Biosystems/MDS Sciex, Foster City, CA) equipped with a Prominence LC system (Shimadzu, Kyoto, Japan), operated in the electron spray ionization mode, was used for the quantification of fluvastatin and rifampicin under conditions described in Supplementary Material Table II. The calibration curves were linear in the range of 3–300 nM. The analytical method was validated in terms of selectivity, linearity (relative error (≤ ±15%), correlation coefficient ($r \geq 0.99$)), precision (≤ 15%), and accuracy (≤ ±19%).

Quantification of Gd-EOB-DTPA by ICP-MS

One-hundred twenty μL of aliquots obtained from the uptake study were protein precipitated by adding 240 μL of acetonitrile, mixed and centrifuged at 15,000 rpm for 5 min. The supernatants (300 μL) were evaporated to dryness at room temperature in a centrifugal concentrator, and then reconstituted in 1 ml of 0.08 N nitric acid containing 2 ppb of ^{115}In (internal standard) followed by ICP-MS analysis. ICP-MS (model SPQ9700; SII NanoTechnology, Seiko) was used for the quantification of Gd-EOB-DTPA. Isotopes monitored were ^{157}Gd and ^{115}In. The calibration curves were linear in the range of 0.1–5 ng/mL (ICP-MS). The analytical method was validated in terms of selectivity, linearity (Relative error (≤±2.5%), correlation coefficient (r): ≥ 0.999), precision (≤ 2.5%), and accuracy (≤±2.5%).

Genomic DNA Extraction and Bisulfite Sequencing

Human tissue specimens were obtained from non-profit organization Human and Animal Bridging Research Organization (Tokyo, Japan). Genomic DNA from each cell line or human tissue specimen was extracted using a Get pure DNA Kit (Dojindo Molecular Technologies, Gaithersburg, MD) according to the manufacturer's instructions. One to two micrograms of genomic DNA was digested with BamHI (Takara) and subjected to the bisulfite reaction as described previously (20). The DNA was then precipitated with ethanol, dried, and resuspended in TE buffer (10 mM Tris–HCl, 1 mM EDTA, pH 8.0). The DNA fragments were amplified by PCR using primers shown in Supplementary Material Table I. The PCR was performed using BIOTAQ^{TM} HS DNA Polymerase (Bioline, London, UK) under the following conditions: 94°C for 10 min; 43 cycles of 94°C for 30 s, 55°C for 30 s, and 72°C for 1 min; final extension 72°C for 10 min. The PCR products were cloned into the pGEM-T Easy vector (Promega, Madison, WI), and 10 clones chosen randomly from each sample were sequenced to determine the presence of methylated cytosines.

5-aza-2′-Deoxycytidine Treatment

HepG2 and Caco-2 cells were plated in 12-well plates at the density of 1.0×10^5 cells/well and precultured for 24 h. Then, cells were cultured for 72 h in medium containing 0, 1, 10, or 100 μM of 5-aza-2′-deoxycytidine (5azadC, Sigma-Aldrich). Expression level of OATP1B3 mRNA was quantified as described above. The fold induction in the mRNA expression by 5azadC treatment was calculated compared with the untreated cells in each cell line.

siRNA Knockdown of Methyl-DNA Binding Proteins (MBDs)

The dsRNAs of MeCP2, MBD1, MBD2, and MBD4 listed in Supplementary Material Table III were purchased from Invitrogen (Carlsbad, CA). The dsRNAs (50 pmol/ml) were transfected into HepG2 or Caco-2 cells by using Lipofectamine 2000 (Invitrogen) according to the manufacturer's instructions, and the cells were cultured for 48 h. mRNA expression of MBDs was quantified by real-time PCR using the primers shown in Supplementary Material Table I (21,22) to examine the knockdown efficiency of three different dsRNAs for each MBD. MeCP2-siRNA-1, MBD1-siRNA-1, MBD2-siRNA-3, and MBD4-siRNA-3 showed the highest reduction in the mRNA expression of respective MBDs in HepG2 and Caco-2 cells (data not shown), and thus selected for subsequent experiments. The fold induction in the mRNA expression of Ct-OATP1B3 by siRNA treatment was calculated compared with the cells treated with negative control siRNA (Invitrogen).

RESULTS

Identification of Transcription Start Site of Ct-OATP1B3 in PK-8 Cells

5′-RACE was performed to identify the TSS of *OATP1B3* in PK-8 cells. 5′-end of the OATP1B3 cDNA sequence obtained

from PK-8 cells was located between exon 2 and exon 3 of *SLCO1B3* gene (Fig. 1a). The TSS of *Ct-OATP1B3* identified in the present study was 20 bp upstream of that reported previously (14), and the exon 1 specific to Ct-OATP1B3 was named exon 1*. The ORF of Ct-OATP1B3 was searched using ORF Finder (http://www.ncbi.nlm.nih.gov/projects/gorf/). The translation start codon was suggested to exist in exon 3, and the translated product was a 674-amino acid polypeptide that lacks the first 28 amino acids at the N-terminal position of Lt-OATP1B3. In addition, another OATP1B3 variant, with a 90 bp insertion between exons 4 and 5 of Ct-OATP1B3 was found in the cDNA from PK-8 cells. The inserted sequence was located about 300 bp downstream of exon 4. However, the translation stop codon was found in the inserted exon, and this variant would produce a 91-amino acid polypeptide (Supplementary Material Fig. 1).

mRNA Expression of OATP1B3 Variants in Cancer Cell Lines and Normal Tissues

The mRNA expression of Lt- and Ct-OATP1B3 in human cancer cell lines (PK-8, PK-45P, DLD-1, TFK-1, HepG2, and Caco-2) and in the human liver and kidney was quantified by real-time PCR (Fig. 1b). The mRNA expression of Ct-OATP1B3 was significantly higher in PK-8, PK-45P, DLD-1, and TFK-1 cells compared with HepG2 and Caco-2 cells. The expression levels of Lt-OATP1B3 in these cell lines were below the limit of quantification. By contrast, Lt-OATP1B3 was the major OATP1B3 variant in human liver, which displayed negligible expression of Ct-OATP1B3. Neither Lt-OATP1B3 nor Ct-OATP1B3 was detected in human kidney.

Subcellular Localization of Ct-OATP1B3 in HEK293 Cells

The subcellular localization of Ct-OATP1B3 in mammalian cells was investigated by immunocytochemistry. HEK293 cells, which lack the endogenous expression of Ct-OATP1B3, were transiently transfected with a plasmid vector containing the cDNA of Ct-OATP1B3 with a FLAG epitope at the C-terminus (p3×FLAG-CMV-14-Ct-OATP1B3). The localization of Ct-OATP1B3 was then examined by immunostaining using polyclonal antibodies against the FLAG epitope and a plasma membrane marker (Na^+, K^+-ATPase alpha 1 subunit) or other subcellular organelle markers (calnexin, endoplasmic reticulum membrane; EEA1, early endosome;

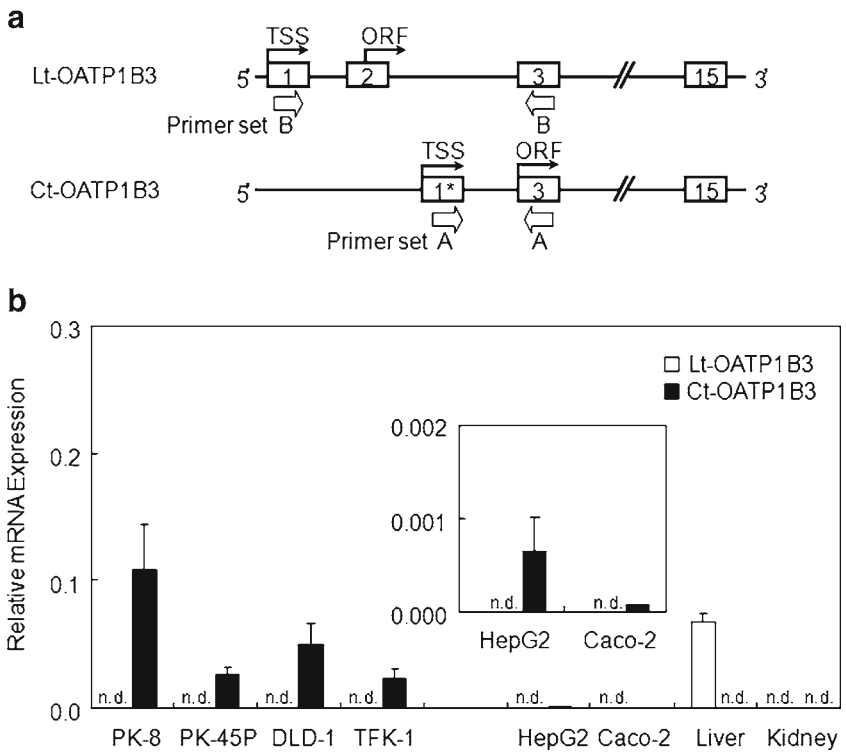

Fig. 1 Identification and cloning of Ct-OATP1B3. (**a**) Exon-intron structure of Ct-OATP1B3. Exons of liver-type (Lt) and cancer-type (Ct) OATP1B3 are indicated by *open boxes*. The position of primer sets were shown by *arrows*. TSS, transcription start site; ORF, open reading frame. (**b**) mRNA expression profiles of OATP1B3 in cancer cell lines and normal tissues. mRNA expression of Lt- and Ct-OATP1B3 were quantified in cancer cell lines (PK-8, PK-45P, DLD-1, TFK-1, HepG2, and Caco-2) and normal tissues (liver and kidney) by real-time PCR using specific primers (Supplementary Material Table 1) as described in Materials and Methods. The mRNA expression levels are represented as a ratio to that of GAPDH in each sample. Each bar represents the mean ± S.E. of triplicate experiments. mRNA expression of Lt-OATP1B3 in HepG2, Caco-2, PK-8, PK-45P, DLD-1, TFK-1, and kidney, that of Ct-OATP1B3 in the liver and kidney was not detected (n.d.).

GM130, cis-Golgi; LAMP-1, lysosome; MitoTracker, mitochondria). Ct-OATP1B3 colocalized with Na^+, K^+-ATPase (Fig. 2a) but not with the other subcellular organelle markers (Supplementary Material Fig. 2a–e). These results suggest that Ct-OATP1B3 localizes predominantly on the plasma membrane when transfected into HEK293 cells.

Transport Activities by Ct-OATP1B3 in HEK293 Cells

The transport activities of Ct-OATP1B3 were investigated using representative substrates of Lt-OATP1B3 including $E_2$17βG, fluvastatin, rifampicin, and Gd-EOB-DTPA. The uptake of these compounds was significantly higher in HEK293T cells transiently transfected with Ct-OATP1B3 compared with mock-transfected cells (Fig. 2b). In addition, 100 μM rifampicin, a known inhibitor of Lt-OATP1B3, inhibited the uptake of $E_2$17βG, fluvastatin and Gd-EOB-DTPA to the level of mock-transfected controls. The uptake of rifampicin was saturated at higher substrate concentration (100 μM) compared with the tracer concentration (0.1 μM). The time-dependent uptake of rifampicin was also observed (Supplementary Material Fig. 3). The results of the uptake study for fluvastatin and rifampicin using Lt-OATP1B3-expressing HEK293 cells (Supplementary Material Fig. 4) were qualitatively similar to those for Ct-OATP1B3.

DNA Methylation Profiles of Ct-OATP1B3 in Cancer Cell Lines and Normal Tissues

Ten CpG dinucleotides were located in the genomic region from 300 bp upstream to 100 bp downstream of the TSS of *Ct-OATP1B3*. The DNA methylation profiles of these CpG dinucleotides were determined in cancer cell lines (PK-8, PK-45P, DLD-1, TFK-1, HepG2, and Caco-2) and in normal human tissues (liver and kidney cortex) (Fig. 3). The CpG dinucleotides from −230 to +93 relative to the TSS of *Ct-OATP1B3* were almost completely hypomethylated in PK-8, PK-45P, DLD-1, and TFK-1 cells, were moderately

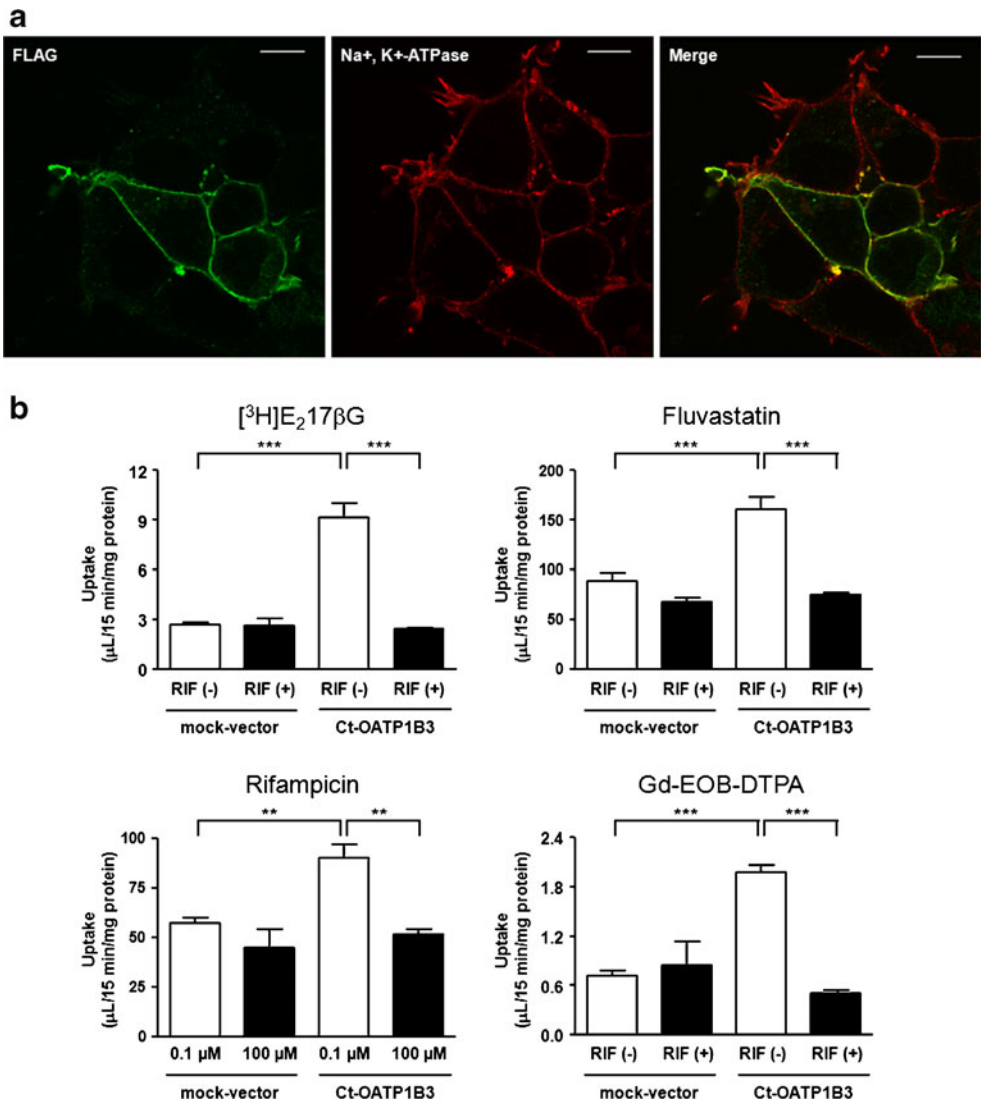

Fig. 2 Subcellular localization and transport activity of Ct-OATP1B3 in HEK293 cells. (**a**) HEK293 cells transfected with p3 × FLAG-CMV-14-Ct-OATP1B3 vector were stained with anti-FLAG antibody (*left panel*, *green*) and anti-Na^+, K^+-ATPase alpha 1 subunit antibody (*middle panel*, *red*) for confocal laser scanning microscopy as described in Materials and Methods. Yellow signals in the merged image (right panel) indicate the colocalization. Scale bar: 10 μm. (**b**) Transport activity of Ct-OATP1B3. Uptake of [^{3}H]$E_2$17βG (0.1 μM), fluvastatin (1 μM), rifampicin (0.1 μM), or Gd-EOB-DTPA (100 μM) for 15 min was determined in HEK293T cells expressing Ct-OATP1B3, and mock vector transfected cells at 37°C in the absence or presence of rifampicin (100 μM). Each bar represents the mean ± S.E. of quadruplicate experiments. Significant differences between the groups were denoted by asterisks (**$P < 0.01$, ***$P < 0.001$; one-way analysis of variance with Tukey's test).

methylated in HepG2 cells, and were almost completely hypermethylated in Caco-2 cells and human liver and kidney cortex. The degree of methylation at −282 and −267 CpG dinucleotides was low to moderate in PK-8, PK-45P, DLD-1, and TFK-1 cells, and almost completely hypermethylated in HepG2 and Caco-2 cells and human liver and kidney cortex.

Effect of DNA Methylation Inhibitor on the mRNA Expression of Ct-OATP1B3

To elucidate the role of DNA methylation in the mRNA expression of OATP1B3, HepG2 and Caco-2 cells, in which the endogenous expression of Lt- or Ct-OATP1B3 was negligible or minimal, were treated with increasing concentrations of 5azadC, an inhibitor of DNA methyltransferase, and the mRNA expression of Lt- and Ct-OATP1B3 was quantified by real-time PCR. Treatment with 5azadC increased the expression of Ct-OATP1B3 in a concentration dependent manner by up to 16- and 32-fold in HepG2 and Caco-2 cells, respectively (Fig. 4). By contrast, the expression of Lt-OATP1B3 remained below the lower limit of quantification in all samples (data not shown).

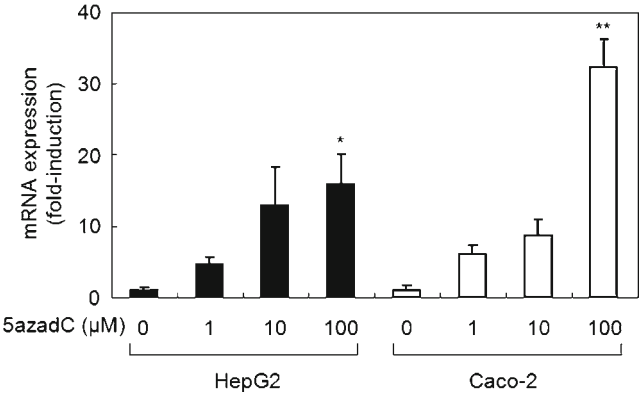

Fig. 4 Effect of DNA methylation inhibitor on the mRNA expression of Ct-OATP1B3. mRNA expression of Ct-OATP1B3 following 5-aza-2′-deoxycytidine (5azadC) treatment. HepG2 and Caco-2 cells were cultured for 72 h with 0, 1, 10, or 100 μM of 5azadC, and then real-time quantitative PCR was performed as described in Materials and Methods. The relative mRNA expression of Ct-OATP1B3 was given as a ratio with respect to that in untreated cells in each cell line. Results are presented as the mean ± S.E. of triplicate experiments. Asterisks indicate significant differences relative to control (*$P < 0.05$, **$P < 0.01$; one-way analysis of variance with Dunnett's test).

Effect of siRNAs Against the Methyl-DNA Binding Proteins on the mRNA Expression of Ct-OATP1B3

MBDs are known to mediate transcriptional repression by binding to methylated CpG dinucleotides. We investigated the roles of MeCP2, MBD1, MBD2, and MBD4, which are well characterized MBDs, in the DNA methylation-dependent gene silencing of Ct-OATP1B3. The mRNA expression of these MBDs was detected in both Ct-OATP1B3-positive (PK-8, PK-45P, DLD-1, and TFK-1) and Ct-OATP1B3-negative (HepG2 and Caco-2) cell lines (Supplementary Material Fig. 5a). There was no clear correlation between the mRNA expression of Ct-OATP1B3 and a particular MBD.

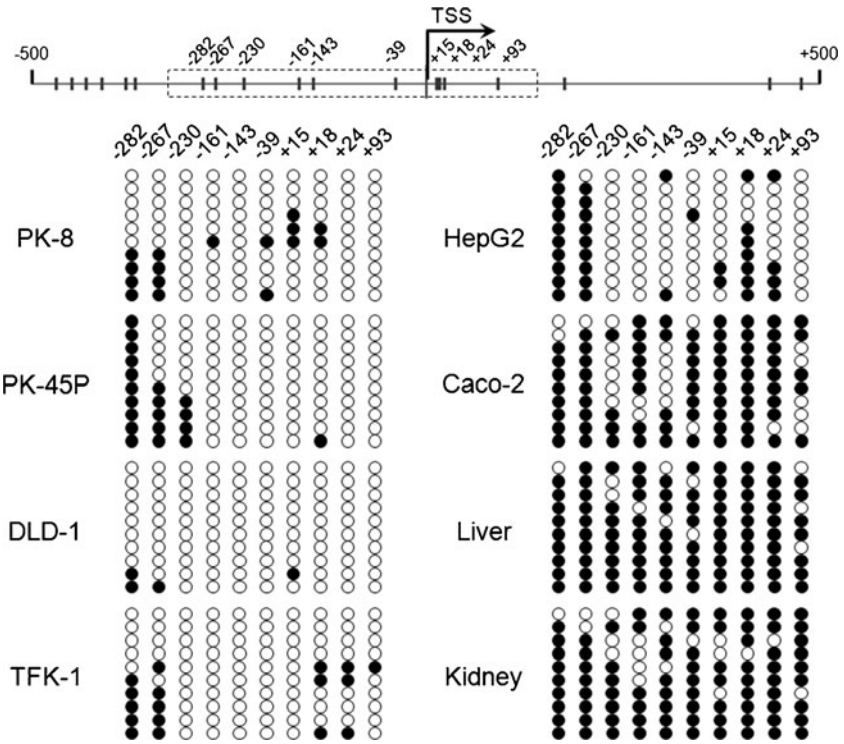

Fig. 3 DNA methylation profiles around the transcriptional start site of *Ct-OATP1B3*. Bisulfite genomic sequencing was performed around the transcriptional start site (TSS) of *Ct-OATP1B3* with genomic DNA extracted from cancer cell lines (PK-8, PK-45P, DLD-1, TFK-1, HepG2, and Caco-2) and normal tissues (liver and kidney cortex) as described in Materials and Methods. Top: Schematic diagrams of the genomic region around the TSS. The vertical lines and numbers indicate the positions of the cytosine residues of CpG dinucleotides relative to the TSS of *Ct-OATP1B3* (+1). Bottom: DNA methylation status of individual CpG dinucleotides. The open and closed circles represent unmethylated and methylated cytosines, respectively.

The effect of siRNA specific for each MBD on the mRNA expression of Ct-OATP1B3 was examined to elucidate the role of individual MBDs. siRNA knockdown of MBD2 significantly increased the mRNA expression of Ct-OATP1B3 in HepG2 and Caco-2 cells, but the effect of other siRNAs was negligible (Fig. 5). The mRNA expression of other MBDs was unaffected by the transfection, confirming the specificity of each dsRNA to its target gene (Supplementary Material Fig. 5b).

DISCUSSION

Ct-OATP1B3 has been identified recently as a predominant OATP1B3 variant in human cancer cell lines and tumors (14,15). The present study characterized the function and epigenetic regulation of Ct-OATP1B3.

The TSS of *OATP1B3* was located in the intron 2 of *SLCO1B3* gene in PK-8 cells (Fig. 1a), a finding that is consistent with recent findings in other cancerous tissues and cells (14,15). The genome-wide analysis using the oligo-capping method in the DataBase of Transcriptional Start Sites (DBTSS; http://dbtss.hgc.jp/) (23) indicated that the most common TSS of *OATP1B3* in DLD-1 cells was located in exon 1*, which is 63 bp downstream of the TSS identified in PK-8 cells. In addition, chromatin immunoprecipitation (ChIP)-Seq analysis in the same database detected RNA polymerase II binding, histone H3K4 trimethylation and H3 acetylation signals around exon 1* in DLD-1 cells (24). These observations are consistent with our findings that the expression of Ct-OATP1B3 is more prevalent in cancer cell lines compared with that of Lt-OATP1B3 (Fig. 1b). It is noteworthy that the translation start codon found in exon 3 of *SLCO1B3* gene by our group and by Thakkar and co-workers is different from that first reported for Ct-OATP1B3 (14). Accordingly, Ct-OATP1B3 is considered a 674-amino acid polypeptide, which lacks the first 28 amino acids in the N-terminus of Lt-OATP1B3. Several studies have reported on the protein expression of OATP1B3 in human cancerous tissues assessed using antibodies against OATP1B3 (6,7,9,25). The epitopes of antibodies used to detect the OATP1B3 protein in gastrointestinal (6), breast (7), and colon (9) cancers were located in the C-terminus of OATP1B3 protein, which is identical between Ct-OATP1B3 and Lt-OATP1B3; thus, the major variant of OATP1B3 in these cancerous tissues remains obscure. However, the predominant mRNA expression of Ct-OATP1B3 in various cancer tissues including colon, lung, and pancreatic cancers indicates its protein expression as the major OATP1B3 variant (14,15). By contrast, Lt-OATP1B3 seems to be the primary variant of OATP1B3 in hepatocellular carcinoma (25), as shown by reaction with the antibody raised against the N-terminal peptide of Lt-OATP1B3, which is absent in Ct-OATP1B3. This could reflect the abundant expression of Lt-OATP1B3 in normal liver before its tumorigenesis or the different use of the TSS in different tumor types.

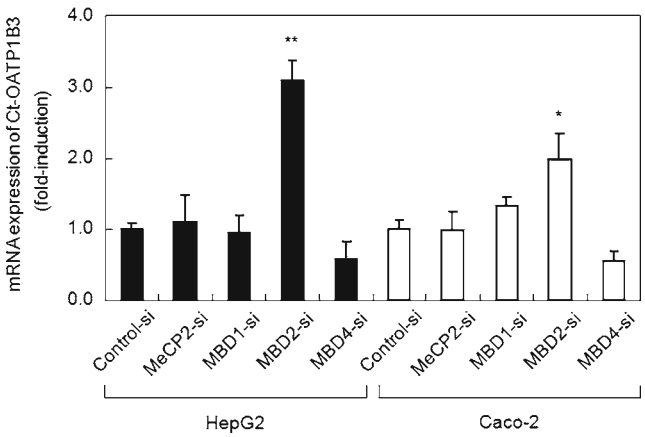

Fig. 5 Involvement of MBD2 in the epigenetic regulation of Ct-OATP1B3. Effect of siRNAs targeted for MBDs on the mRNA expression of Ct-OATP1B3. HepG2 and Caco-2 cells were transfected with siRNAs (50 pmol/ml), cultured for 48 h, and then real-time quantitative PCR was performed as described in Materials and Methods. The fold induction in the mRNA expression by siRNA treatment was calculated compared with the cells treated with negative control siRNA. Results are presented as the mean ± S.E. of triplicate experiments. Asterisks indicate significant differences relative to control (*$P < 0.05$, **$P < 0.01$; one-way analysis of variance with Dunnett's test).

Based on its amino acid sequence, it was predicted that Ct-OATP1B3 likely possesses 12 transmembrane domains, which is typical for membrane transporters in the SLCO family, which is capable of transporting various substrates (2). Further studies are warranted to confirm whether there are 12 transmembrane domains. To investigate the subcellular localization and transport function of Ct-OATP1B3, a plasmid vector containing the proposed ORF of Ct-OATP1B3 was constructed and transiently transfected into HEK293 cells. Ct-OATP1B3 localized predominantly on the plasma membrane in HEK293 cells, and showed significant transport activities for the four representative substrates of Lt-OATP1B3 (Fig. 2a and b). These results suggest that Ct-OATP1B3 acts as a membrane transporter when overexpressed in tumor-derived cell lines. Lee and co-workers reported that overexpression of Lt-OATP1B3 in colorectal cancer cells, but not its mutant form with impaired transport activity, confers an antiapoptotic advantage by altering the p53-dependent pathways, although the underlying mechanism has yet to be determined. The fact that Ct-OATP1B3 maintains its transport activity indicates that the endogenous expression of Ct-OATP1B3 may result in the same outcome. By contrast, immunoreactivity of OATP1B3 and its haplotype is associated with an improved prognosis in breast and prostate cancer, respectively (7,10). The mechanism underlying these apparently contradictory observations remains unclear. It is known that the substrates of Lt-OATP1B3 include endogenous compounds such as steroid and thyroid hormones and eicosanoids (2). We have

demonstrated that Ct-OATP1B3 shares at least some substrate specificity with Lt-OATP1B3. It is possible that Ct-OATP1B3-mediated accumulation of endogenous hormones differentially affects the downstream signaling pathways depending on the origin of the tumor. It may also be worthwhile to pursue the use of Ct-OATP1B3 in cancer diagnostics. In addition to the conventional immunostaining method, the functional expression of Ct-OATP1B3 could be examined by positron emission tomography using [^{11}C]telmisartan or magnetic resonance imaging (MRI) using Gd-EOB-DTPA because these compounds are substrates of Lt- and/or Ct-OATP1B3 (25,26). Further studies are warranted to elucidate the biological relevance of OATP1B3 in cancer tissues and its potential application in cancer chemotherapy.

Bisulfite sequencing and real-time PCR analysis demonstrated that the DNA methylation status of CpG dinucleotides around the TSS of *Ct-OATP1B3* is consistent with its mRNA expression (Figs. 1b and 3); that is, with the overall hypermethylated status in Ct-OATP1B3-negative cell lines (HepG2 and Caco-2) and in normal liver and kidney cortex, but with the completely hypomethylated status in Ct-OATP1B3-positive cell lines (PK-8, PK-45P, DLD-1, and TFK-1). Furthermore, treatment with 5azadC, a DNA methylation inhibitor, significantly increased the mRNA expression of Ct-OATP1B3, but not of Lt-OATP1B3, in the cell lines in which its endogenous expression is minimal or negligible (Fig. 4). These results suggest that DNA methylation is involved in the regulation of Ct-OATP1B3 expression. Future studies should determine the mRNA expression and DNA methylation profiles of Ct-OATP1B3 in clinical tumor samples. MBDs are crucial in DNA methylation-dependent gene silencing, during which these proteins bind to methylated CpG dinucleotides and recruit the transcriptional repressor complex (27,28). Among MBD proteins, MBD2 appears to have the greatest effect on gene silencing in cancer cells (29). More recently, whole-genome mapping using ChIP combined with human promoter tiling arrays has shown the preferential localization of MBD2 near TSSs in HeLa cells (30). siRNA-induced knockdown of MBD2, but not of other MBDs, stimulates the expression of Ct-OATP1B3 (Fig. 5). It is likely that the epigenetic regulation of Ct-OATP1B3 involves MBD2 in cancer cells.

We previously observed an apparent discrepancy between the DNA methylation status and mRNA expression of OATP1B3 in PK-8 and PK-45P cells (12); the four CpG dinucleotides around the TSS were hypomethylated in these two cell lines despite the abundant expression of OATP1B3. This can be explained by the fact that the primers used to determine the mRNA expression of OATP1B3 in our previous study were designed against the common sequence between Lt-OATP1B3 and Ct-OATP1B3, and we examined the DNA methylation status around the TSS of *Lt-OATP1B3*. The present study shows that PK-8 and PK-45P cells use the alternative TSS around which the CpG dinucleotides are almost completely hypomethylated, which is consistent with the preferential transcription of Ct-OATP1B3. We also demonstrated that the same four CpG dinucleotides neighboring the TSS of *Lt-OATP1B3* are differentially methylated in human liver and kidney in a manner consistent with the liver-specific expression (13). Taken together, those findings suggest that DNA methylation determines the distinct usage of tissue- and cell type-specific TSSs, which leads to the predominant expression of the corresponding OATP1B3 variant (Fig. 6). Along with DNA methylation, microRNAs or unidentified transcription factors might act as fine-tune regulators of the transcription of Ct-OATP1B3. MicroRNAs sometimes cause histone modification and DNA methylation of promoter sites, affecting the expression of target genes (31,32). It is possible

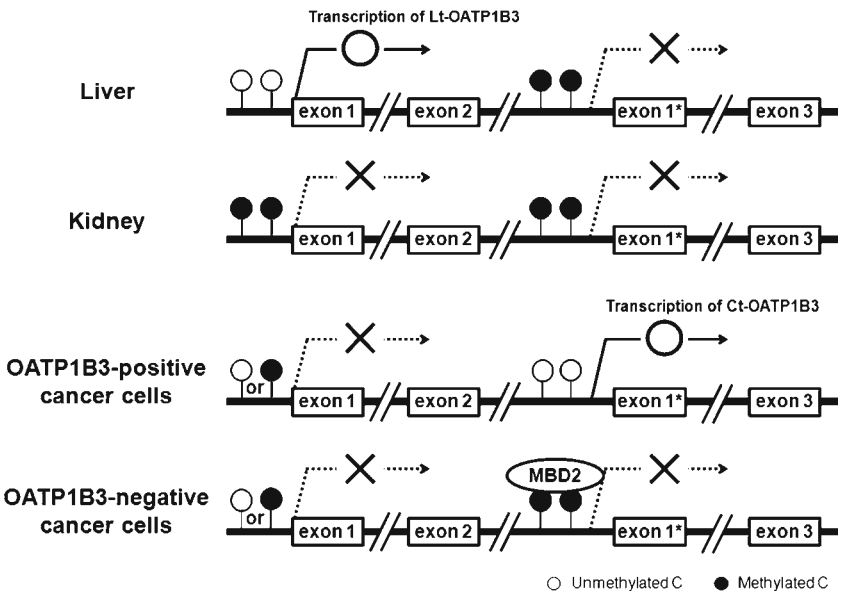

Fig. 6 Proposed mechanism underlying the transcriptional regulation of the cell- and tissue-specific expression of OATP1B3. Both cell- and tissue-specific expression of the corresponding OATP1B3 variant are likely regulated by DNA methylation. See text for details.

that site-specific DNA methylation of Ct-OATP1B3 or Lt-OATP1B3 is regulated by microRNAs.

In conclusion, the present study provides a clear demonstration that Ct-OATP1B3 retains a transport function similar to that of Lt-OATP1B3, and that its ectopic expression is regulated by DNA methylation-dependent gene silencing involving MBD2.

ACKNOWLEDGMENTS AND DISCLOSURES

We thank Yuko Shiono and Yuta Shibue for their excellent technical assistance.

This study was supported by the Japan Society for the Promotion of Science [Grant-in-Aid for Scientific Research (S) 24229002, Scientific Research (B) 23390034, and Grant-in-Aid for Challenging Exploratory Research 21659037].

REFERENCES

1. Giacomini KM, Huang SM, Tweedie DJ, Benet LZ, Brouwer KL, Chu X, *et al.* Membrane transporters in drug development. Nat Rev Drug Discov. 2010;9(3):215–36.
2. Hagenbuch B, Gui C. Xenobiotic transporters of the human organic anion transporting polypeptides (OATP) family. Xenobiotica. 2008;38(7–8):778–801.
3. Maeda K, Sugiyama Y. Impact of genetic polymorphisms of transporters on the pharmacokinetic, pharmacodynamic and toxicological properties of anionic drugs. Drug Metab Pharmacokinet. 2008;23(4):223–35.
4. Yoshida K, Maeda K, Sugiyama Y. Hepatic and intestinal drug transporters: prediction of pharmacokinetic effects caused by drug-drug interactions and genetic polymorphisms. Annu Rev Pharmacol Toxicol. 2012.
5. van de Steeg E, Stranecky V, Hartmannova H, Noskova L, Hrebicek M, Wagenaar E, *et al.* Complete OATP1B1 and OATP1B3 deficiency causes human Rotor syndrome by interrupting conjugated bilirubin reuptake into the liver. J Clin Invest. 2012;122(2):519–28.
6. Abe T, Unno M, Onogawa T, Tokui T, Kondo TN, Nakagomi R, *et al.* LST-2, a human liver-specific organic anion transporter, determines methotrexate sensitivity in gastrointestinal cancers. Gastroenterology. 2001;120(7):1689–99.
7. Muto M, Onogawa T, Suzuki T, Ishida T, Rikiyama T, Katayose Y, *et al.* Human liver-specific organic anion transporter-2 is a potent prognostic factor for human breast carcinoma. Cancer Sci. 2007;98(10):1570–6.
8. Monks NR, Liu S, Xu Y, Yu H, Bendelow AS, Moscow JA. Potent cytotoxicity of the phosphatase inhibitor microcystin LR and microcystin analogues in OATP1B1- and OATP1B3-expressing HeLa cells. Mol Cancer Ther. 2007;6(2):587–98.
9. Lee W, Belkhiri A, Lockhart AC, Merchant N, Glaeser H, Harris EI, *et al.* Overexpression of OATP1B3 confers apoptotic resistance in colon cancer. Cancer Res. 2008;68(24):10315–23.
10. Hamada A, Sissung T, Price DK, Danesi R, Chau CH, Sharifi N, *et al.* Effect of SLCO1B3 haplotype on testosterone transport and clinical outcome in caucasian patients with androgen-independent prostatic cancer. Clin Cancer Res. 2008;14(11):3312–8.
11. Svoboda M, Wlcek K, Taferner B, Hering S, Stieger B, Tong D, *et al.* Expression of organic anion-transporting polypeptides 1B1 and 1B3 in ovarian cancer cells: relevance for paclitaxel transport. Biomed Pharmacother. 2011;65(6):417–26.
12. Ichihara S, Kikuchi R, Kusuhara H, Imai S, Maeda K, Sugiyama Y. DNA methylation profiles of organic anion transporting polypeptide 1B3 in cancer cell lines. Pharm Res. 2010;27(3):510–6.
13. Imai S, Kikuchi R, Kusuhara H, Sugiyama Y. DNA methylation and histone modification profiles of mouse organic anion transporting polypeptides. Drug Metab Dispos. 2013;41(1):72–8.
14. Nagai M, Furihata T, Matsumoto S, Ishii S, Motohashi S, Yoshino I, *et al.* Identification of a new organic anion transporting polypeptide 1B3 mRNA isoform primarily expressed in human cancerous tissues and cells. Biochem Biophys Res Commun. 2012;418(4):818–23.
15. Thakkar N, Kim K, Jang ER, Han S, Kim D, Merchant N, Lockhart AC, Lee W. A cancer-specific variant of the SLCO1B3 gene encodes a novel human organic anion transporting polypeptide 1B3 (OATP1B3) localized mainly in the cytoplasm of colon and pancreatic cancer cells. Mol Pharm. 2013;10(1):406–16.
16. Obaidat A, Roth M, Hagenbuch B. The expression and function of organic anion transporting polypeptides in normal tissues and in cancer. Annu Rev Pharmacol Toxicol. 2012;52:135–51.
17. Kikuchi R, Kusuhara H, Hattori N, Shiota K, Kim I, Gonzalez FJ, *et al.* Regulation of the expression of human organic anion transporter 3 by hepatocyte nuclear factor 1alpha/beta and DNA methylation. Mol Pharmacol. 2006;70(3):887–96.
18. Hirano M, Maeda K, Shitara Y, Sugiyama Y. Contribution of OATP2 (OATP1B1) and OATP8 (OATP1B3) to the hepatic uptake of pitavastatin in humans. J Pharmacol Exp Ther. 2004;311(1):139–46.
19. Lowry OH, Rosebrough NJ, Farr AL, Randall RJ. Protein measurement with the Folin phenol reagent. J Biol Chem. 1951;193(1):265–75.
20. Kikuchi R, Kusuhara H, Hattori N, Kim I, Shiota K, Gonzalez FJ, *et al.* Regulation of tissue-specific expression of the human and mouse urate transporter 1 gene by hepatocyte nuclear factor 1 alpha/beta and DNA methylation. Mol Pharmacol. 2007;72(6):1619–25.
21. Saito Y, Kanai Y, Sakamoto M, Saito H, Ishii H, Hirohashi S. Expression of mRNA for DNA methyltransferases and methyl-CpG-binding proteins and DNA methylation status on CpG islands and pericentromeric satellite regions during human hepatocarcinogenesis. Hepatology. 2001;33(3):561–8.
22. Huntriss J, Hinkins M, Oliver B, Harris SE, Beazley JC, Rutherford AJ, *et al.* Expression of mRNAs for DNA methyltransferases and methyl-CpG-binding proteins in the human female germ line, preimplantation embryos, and embryonic stem cells. Mol Reprod Dev. 2004;67(3):323–36.
23. Suzuki Y, Yamashita R, Nakai K, Sugano S. DBTSS: DataBase of human transcriptional start sites and full-length cDNAs. Nucleic Acids Res. 2002;30(1):328–31.
24. Yamashita R, Sathira NP, Kanai A, Tanimoto K, Arauchi T, Tanaka Y, *et al.* Genome-wide characterization of transcriptional start sites in humans by integrative transcriptome analysis. Genome Res. 2011;21(5):775–89.
25. Narita M, Hatano E, Arizono S, Miyagawa-Hayashino A, Isoda H, Kitamura K, *et al.* Expression of OATP1B3 determines uptake of Gd-EOB-DTPA in hepatocellular carcinoma. J Gastroenterol. 2009;44(7):793–8.
26. Shimizu K, Takashima T, Yamane T, Sasaki M, Kageyama H, Hashizume Y, *et al.* Whole-body distribution and radiation dosimetry of [11C]telmisartan as a biomarker for hepatic organic anion transporting polypeptide (OATP) 1B3. Nucl Med Biol. 2012;39(6):847–53.

27. Clouaire T, Stancheva I. Methyl-CpG binding proteins: specialized transcriptional repressors or structural components of chromatin? Cell Mol Life Sci. 2008;65(10):1509–22.
28. Bogdanovic O, Veenstra GJ. DNA methylation and methyl-CpG binding proteins: developmental requirements and function. Chromosoma. 2009;118(5):549–65.
29. Lopez-Serra L, Ballestar E, Ropero S, Setien F, Billard LM, Fraga MF, *et al.* Unmasking of epigenetically silenced candidate tumor suppressor genes by removal of methyl-CpG-binding domain proteins. Oncogene. 2008;27(25):3556–66.
30. Chatagnon A, Perriaud L, Nazaret N, Croze S, Benhattar J, Lachuer J, *et al.* Preferential binding of the methyl-CpG binding domain protein 2 at methylated transcriptional start site regions. Epigenetics. 2011;6(11).
31. Hawkins PG, Morris KV. RNA and transcriptional modulation of gene expression. Cell Cycle. 2008;7(5):602–7.
32. Tan Y, Zhang B, Wu T, Skogerbo G, Zhu X, Guo X, *et al.* Transcriptional inhibiton of Hoxd4 expression by miRNA-10a in human breast cancer cells. BMC Mol Biol. 2009; 10:12.